Preserving Nearly Diffraction-Limited Beam Quality Over Several Hundred Meters of Transmission Through Highly Multimode Fibers

Christian Röhrer, Christophe A. Codemard, *Senior Member, OSA*, Götz Kleem, Thomas Graf, and Marwan Abdou Ahmed

***Abstract*—The influence of the core diameter and the fiber length on the beam quality of the transmitted beam was investigated theoretically and experimentally for highly multimode step-index fibers with a numerical aperture of 0.22 using a fully monolithic setup. We show that it is possible to maintain a nearly diffraction-limited beam quality ($M^2 \approx 1.3$) through 100 m long multimode fibers. For a core diameter of 60 μm and a fiber length of 380 m one can still deliver a beam with an M^2 value of 2.1. The high-power suitability of this approach was shown by transmitting 1 kW of power through a 100 m long fiber with a core diameter of 60 μm without the onset of stimulated Raman scattering while maintaining a nearly diffraction-limited beam quality ($M^2 \approx 1.3$).**

***Index Terms*—Large mode area (LMA), multimode step-index fiber, nearly diffraction-limited beam, stimulated Raman scattering (SRS).**

I. Introduction

FOR laser materials processing optical fibers offer a flexible solution for transporting the laser beam from the laser source to the work piece. The fiber delivery of high-brightness solid-state laser radiation is however limited by to the onset of nonlinear effects. The output of industrial high-power cw fiber lasers typically exhibits a broad spectral bandwidth [1], thus the dominant nonlinearity in the delivery fibers is stimulated Raman scattering (SRS) [2]. The threshold power leading to SRS is proportional to the ratio between the effective mode field area and the fiber length [3]. To overcome SRS and enable the fiber-optic transmission of high-power laser beams over long distances the core size must be enlarged, thus making the fiber multimode. Several approaches have been proposed to mitigate the excitation of higher-order modes and still maintain a diffraction-limited beam along the propagation through fibers with large core diameters, e.g. by introducing high propagation losses for higher-order modes such as in photonic crystal fibers or lowering the numerical aperture (NA) to keep the fiber truly single-mode [4]. These fiber designs are complex, expensive, and very often impractical for flexible beam delivery in industrial applications, because they suffer from excess propagation loss and strong bend-sensitivity. There is still a need for more simple, readily useable, and low-cost solutions to transport high-power beams with good beam quality over several tens to hundreds of meters of fiber.

In the present work we propose to use conventional step-index fibers, which have advantages such as low complexity, low loss, low price, and well-established manufacturing and handling technologies (e.g. cleaving, splicing and tapering). Several groups have already shown the possibility to maintain a diffraction-limited beam along the propagation through multimode fibers with core diameters of a few hundred micrometers and short fiber lengths of several tens of centimeters to up to two meters [5], [6], with core diameters of some tens of micrometers and fiber lengths of ten to twenty meters [7]–[9], or in few-mode fibers with a length of hundred meters or more [10]–[12]. These results show that there is a tradeoff between the size of the core and the length of the fiber.

The aim of the present work was to advance the use of large core diameters together with high numerical apertures while at the same time using long fibers and preserving a nearly diffraction-limited beam quality. The conditions required to preserve a good beam quality along several hundred meters in highly multimode fibers is shown both theoretically and experimentally and is demonstrated by the beam delivery of nearly diffraction-limited laser beams with a power of up to 1 kW. The used fiber-optic beam delivery was set up in a fully monolithic arrangement to allow for power scaling by avoiding the problems caused by thermally induced degradations normally present in free-space optical launching systems. The monolithic approach also provides superior excitation of the fundamental mode in the fiber as compared to a free-space launching, where the free-space Gaussian mode cannot be matched exactly to the fundamental LP_{01}-mode of the fiber [13].

Manuscript received January 22, 2019; revised May 16, 2019; accepted June 4, 2019. Date of publication June 13, 2019; date of current version August 16, 2019. This work was supported by the Deutsche Forschungsgemeinschaft—GSC 262/2. *(Corresponding author: Christian Röhrer.)*

C. Röhrer is with the Institut für Strahlwerkzeuge, University of Stuttgart, 70569 Stuttgart, Germany, and also with the Graduate School of Excellence advanced Manufacturing Engineering, University of Stuttgart, 70569 Stuttgart, Germany (e-mail: christian.roehrer@ifsw.uni-stuttgart.de).

C. A. Codemard is with the Advanced Laser Laboratory, SPI Lasers UK Ltd, Southampton SO30 2QU, U.K. (e-mail: christophe.codemard@spilasers.com).

G. Kleem, T. Graf, and M. Abdou Ahmed are with the Institut für Strahlwerkzeuge, University of Stuttgart, 70569 Stuttgart, Germany (e-mail: goetz.kleem@ifsw.uni-stuttgart.de; thomas.graf@ifsw.uni-stuttgart.de; marwan.abdou-ahmed@ifsw.uni-stuttgart.de).

Color versions of one or more of the figures in this paper are available online at http://ieeexplore.ieee.org.

Digital Object Identifier 10.1109/JLT.2019.2922776

II. Coupled Mode Theory

The degradation of the beam quality occurring along the propagation of the beam in multimode fibers results from a power transfer from the fundamental to higher-order modes. In a perfect waveguide operating in a regime where nonlinear effects are negligible there is no intrinsic mode coupling between the modes. In real fibers the coupling between modes is usually induced by deviations from the ideal waveguide geometry, such as changes of the fiber cross-section along the fiber, variations of the profile of the refractive index or fiber bends [14].

Mode coupling in general can be described using a field coupling model [15], which can be simplified to a power coupling model [16]–[18], as for most cases it is sufficient to consider the power evolution in each mode [19]. It was shown by Marcuse [20] that coupling between two modes only takes place when the suffered perturbation contains a spatial frequency component that is equal to the difference of the propagation constants of the modes, which is proportional to the difference Δn_{eff} of the effective refractive index - or mode spacing - of the two modes. Hence almost degenerate modes with a small Δn_{eff} couple when the perturbation has a low spatial frequency whereas non-degenerate modes - such as the fundamental LP_{01}-mode and higher-order modes - couple when the spatial frequencies of the perturbations are high [19]. The strength of the coupling is proportional to the power spectrum of the curvature along the fiber [21] and depends on the overlap of the field distributions of the two modes and their interaction length [15]. Coupling between adjacent modes is dominant and decreases quickly with increasing mode spacing [18], because for most random perturbations the magnitude of the power spectrum is strongly decreasing with increasing frequency [14], [21]–[23]. Therefore a large Δn_{eff} between LP_{01} and LP_{11} is needed to suppress a power transfer between these modes.

The perturbations at high spatial frequencies are typically induced by microscopic random bends of the waveguide introduced by external stress and are usually referred to as microbending [14]. Mode coupling due to microbending is a stochastic process where the perturbation is considered to be randomly distributed along the fiber [23]. To study these random perturbations along the fiber Olshansky [21] proposed a model assuming an infinite number of small bumps which deform the fiber. Fermann [7] used this model to derive a simple analytical equation to estimate the mode coupling between LP_{01} and LP_{11}, leading to a coupling coefficient d_{12}

$$d_{12} \propto \frac{d_{\text{core}}^8}{d_{\text{clad}}^6 \cdot \lambda^4}, \tag{1}$$

where the indices 1 and 2 correspond to the LP_{01} and the LP_{11} mode, respectively, d_{core} is the core diameter, d_{clad} the cladding diameter and λ the wavelength. At a given wavelength this equation shows that to decrease the coupling between modes due to microbending one has to either reduce the core diameter or to increase the overall fiber thickness and therefore the rigidity of the fiber. Hence, when a large core is needed to suppress SRS, the cladding diameter has to be increased to mitigate mode coupling induced by microbending.

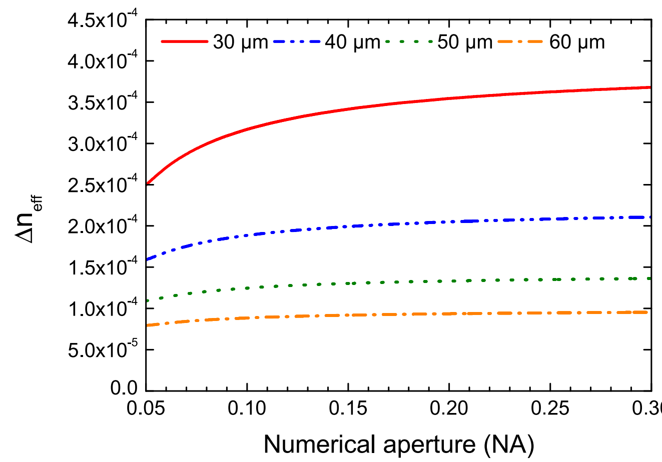

Fig. 1. Calculated Δn_{eff} between LP_{01} and LP_{11} at a wavelength of 1070 nm as function of the NA for core diameters ranging from 30 to 60 μm.

III. Fiber Design

With the above summary of the coupled mode theory as a framework it is now straight forward to design a fiber, which is suitable to preserve diffraction-limited beam quality over long distances. There are two main points that are important for the fiber design to prevent mode coupling, the reduction of perturbations that can lead to mode coupling and the increase of the mode spacing. For the latter numerical simulations based on the finite element method (FEM) were performed to show the dependence of the mode spacing Δn_{eff} on the core diameter and the numerical aperture, which are the two design parameters of a step-index fiber.

Fig. 1 shows the results of these simulations which were performed by solving the Helmholtz equation using the commercially available software COMSOL Multiphysics. It is obvious that the difference Δn_{eff} of the effective refractive indices of the two modes decreases rapidly with increasing core diameter, which is contrary to the need of a large Δn_{eff} to reduce mode coupling. The simulation also shows that Δn_{eff} is almost constant for large NAs, which means that the mode coupling is nearly independent of the numerical aperture when this is sufficiently large, which was already experimentally verified by Hurand *et al* [6]. Furthermore, it is known that the bending sensitivity decreases with increasing NA [4]. For our analysis we have therefore chosen a numerical aperture of 0.22, since this is commercially available and represents the standard in fiber-optics and guarantees a high uniformity of the preform and the drawn fibers. With this NA the number of supported fiber modes amounts to 188, 344, 538 and 762 (including polarization degeneracy) for the fibers with core diameters of 30, 40, 50 and 60 μm, respectively, which highlights that these fibers are indeed highly multimode.

The second goal of the fiber design is the reduction of perturbations that can lead to mode coupling. Therefore, any imperfections in the profile of the refractive index have to be prevented as much as possible. For this we have selected a core made of pure silica with a fluorine-doped cladding. This has the advantage to ensure a significantly more uniform profile of the refractive index, as compared to germanium-doping of the core, which typically exhibits a non-uniform refractive index profile owing to the fabrication process [24].

According to Eq. (1) a large cladding thickness is important to reduce mode coupling. This was confirmed qualitatively by Hurand *et al.* [6], which have shown that the beam quality factor M^2 is reciprocally proportional to the size of the cladding. Furthermore, by increasing the thickness of the cladding by a factor of two, i.e. by changing the ratio between the diameters of core and cladding from 1:2.5 to 1:5.6, Fermann [7] also showed that the propagation length of a single-mode beam can be increased by two orders of magnitude. We therefore used fibers with a ratio $d_{\mathrm{core}}/d_{\mathrm{clad}}$ of 1:6 for our investigations.

IV. Fiber Production

Point defects in the preform as a source of mode coupling can be neglected, since due to the large draw-down ratio in the fiber [24], these imperfections will stretch and related perturbations will belong to the low-frequency regime [14]. Based on the combination of fast drawing speeds and a slow thermomechanical response of the glass preform [25], perturbations caused by drawing-induced diameter fluctuations will also fall into the low-frequency regime [14]. Based on the above design considerations, the preform was produced by the commercial provider CeramOptec. Subsequent drawing was conducted using our own drawing facility, where we have drawn fibers with core diameters of 30, 40, 50 and 60 μm with fiber lengths of 100, 180, 300 and 380 m, respectively.

To protect the drawn fibers from mechanical stress and ensure mechanical stability a polymer coating is applied during the drawing process [24]. It is known that microbending can be reduced by decreasing the quotient of the Young's moduli of this encapsulating material and the fiber itself [21]. Typically the Young's modulus of numerous encapsulating plastic materials is three orders of magnitudes smaller than the one of fused silica [26] leading to a strong reduction of microbending. In order to lower microbending, while at the same time ensuring a high mechanical reliability, most optical fiber coatings consist of a double-layer structure [24]. The inner primary coating is made of a soft material, whereas the outer secondary coating is made of a hard material [27]. The primary coating works as a buffer layer and high spatial frequencies are absorbed, therefore this coating acts as a low-pass filter to external perturbations [28], hence reducing the impact of microbending. The secondary coating protects the primary coating and the overall fiber against any mechanical damage [27]. In a numerical study Yang *et al.* [29] have analyzed the influence of the fiber coating on microbending. They concluded that to reduce microbending one has to increase the thickness and the elasticity of the primary coating and decrease the elasticity of the secondary coating. Hence, for our experiments OF-136 from MY Polymers was used as primary coating, having a low refractive index to make the fibers suitable for high-power applications and DeSolite DS-2015 from DSM was applied as secondary coating.

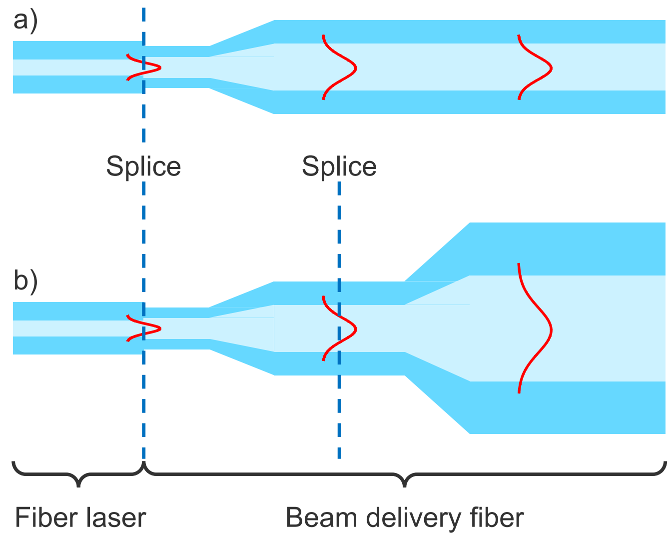

Fig. 2. Layout of the investigated fiber configurations using a fully monolithic arrangement. (a) Configuration for the fiber with a core diameter of 30 μm. (b) Configuration for fibers with core diameters of 40, 50 and 60 μm including an intermediate taper.

As sketched in Fig. 2, a fully monolithic setup with integrated mode field adapters, i.e. so called tapers, to match the modes of the fiber laser and the beam delivery fibers was chosen for the experimental demonstration. For the smallest core diameter of 30 μm the fiber was drawn in one step including the taper (see Fig. 2(a)), whereas for core diameters of 40, 50 and 60 μm the fibers were tapered down to 30 μm in a first step and an additional intermediate taper was needed (see Fig. 2(b)), because the difference between the core diameters of the fiber laser and the beam delivery fiber was too large to ensure a controlled drawing of the corresponding taper in one single step.

To achieve the best overlap between the LP_{01}-mode of the fiber laser and the one at the entrance of the tapered beam delivery fiber, simulations were conducted using the software FIMMWAVE and the included module FIMMPROP. This software package from Photon Design computes a fully vectorial solution of Maxwell's equations. It was found that with the given fiber laser with a core diameter of 15 μm an optimum overlap of 99.3% is achieved when the core diameter at the entrance of the taper of the delivery fiber was chosen to be 18.2 μm. Hence the fibers were drawn with a core diameter of 18.2 μm at the entrance of the tapered section.

A change of the core diameter as a consequence of the integrated mode field adapters, can be understood as a perturbation, but when the change is slow along the propagation distance the mode size adjusts itself adiabatically [30] to follow the changing geometrical dimensions [31]. To fulfill this adiabatic condition the length of the taper has to be sufficiently long or the taper angle has to be sufficiently small [32]. In other words, the transition length of the taper has to be much larger than the coupling length, which is defined as the beat length between two modes, everywhere along the taper [33]. The coupling length is typically in the order of several millimeter to centimeters, which was confirmed by further simulations with FIMMWAVE, where we

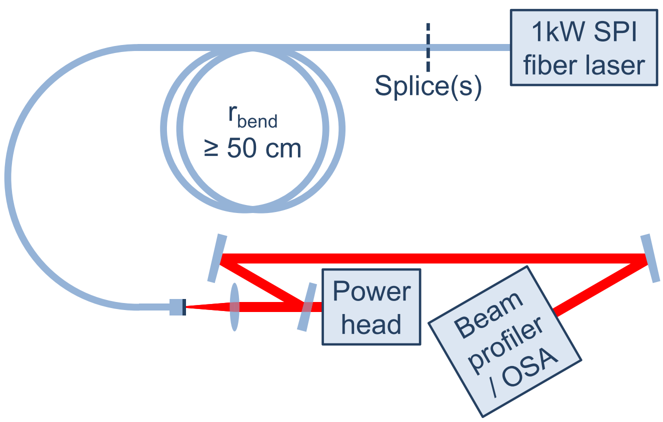

Fig. 3. Experimental setup consisting of a 1 kW cw fiber laser from SPI Lasers with an emission wavelength of 1070 nm and an unpolarized and diffraction-limited output beam. The passive delivery fiber including taper was spliced to the fiber under test (refer to Fig. 2 for details on the layout of each fiber) and the fiber was terminated with an AR-coated end-cap. The beam emitted from the rear side of the delivery fiber was analyzed with respect to power, beam quality, and spectrum.

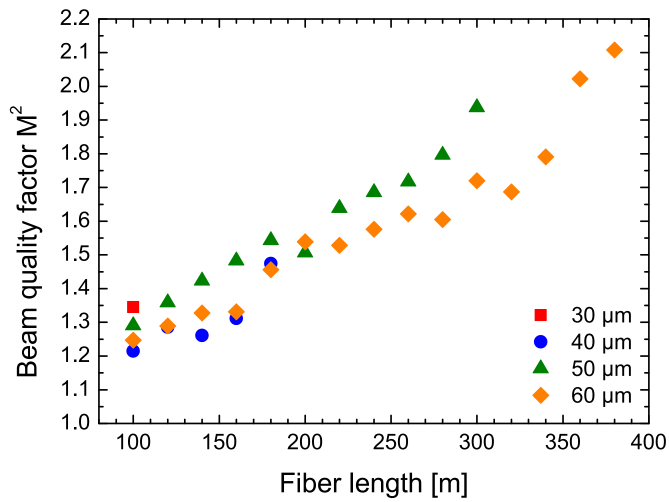

Fig. 4. Measured beam quality factor M^2 as function of the fiber length for the fibers with core diameters of 30, 40, 50 and 60 μm (for the sake of clarity no error bars are shown but the measurement accuracy was $\pm$ 5%).

evaluated the minimum length of the tapers for which no power is transferred from the LP_{01} to any higher-order modes. The produced taper length of 4 m is much longer than the coupling length, which ensured an adiabatic transition of the fundamental mode.

V. Experimental Results

Fig. 3 shows the experimental setup. An unpolarized cw single-mode fiber laser from SPI Lasers, providing a maximum output power of 1 kW at a wavelength of 1070 nm, was spliced to the fibers under test including the tapered sections. All splices were optimized beforehand using a fractional factorial design of experiments for the four main splice parameters: splice power, splice time, overlap and hot push delay [34]. The transmitted power and the beam quality resulting behind the splice were measured during the optimization process. The splice parameters after each run of experiments were adapted until the best parameters were found to minimize power loss, light propagating in the fiber cladding, and the beam quality factor M^2 of the transmitted beam. The splices were placed on water-cooled V-groove fiber holders to reduce bending and were embedded within a polymer with low refractive index. The fiber itself was loosely wound around a fiber spool with a bending radius of approximately 50 cm to minimize microbending. An AR-coated end-cap at the output facet of the fiber was used to mitigate back-reflections into the laser and to increase the beam size in order to reduce the intensity at the interface between glass and air. The beam transmitted through the fiber was analyzed with respect to power, beam quality, and the optical spectrum.

The large bending radius of the fiber ($\geq$50 cm) was used, since the threshold power leading to stimulated Raman scattering is proportional the effective mode field area [3]. As tight fiber bends lead to a reduction of the effective mode field area this also lowers the SRS threshold and should therefore be avoided. The impact of this macroscopic bending on the mode coupling, however, is negligible, which was already reported in [9], where it was shown for similar fibers that the beam quality barely degrades with decreasing bending radius down to a few centimeters.

Fig. 4 shows the measured M^2 values of the beam transmitted through the fibers with various core diameters and as a function of the fiber length. This length refers to the fiber length without the tapered sections. These measurements were performed with a laser power of 50 W. The measurements with different lengths of the fibers were obtained by cutting the fibers back in steps of 20 m until a length of 100 m was reached. The results show that the beam quality degrades with increasing fiber length with a minor influence from the core diameter. However, the observed degradation is moderate. The beam quality factor M^2 of the beam transmitted through 380 m of the fiber with a core diameter of 60 μm, for instance, does not exceed 2.1, which indicates a reasonably limited mode coupling to higher-order modes. A nearly diffraction-limited beam with $M^2 \approx 1.3$ can be preserved for the fibers with a length of around 100 m. This M^2 value is about one order of magnitude smaller than the nominal beam quality factor supported by the tested multimode fibers. The nominal beam quality factor M^2 of the fibers can be estimated by considering their full NA and assuming that all modes of the fiber are equally excited [35]. For the investigated fibers this nominal M^2 factor amounts to 9.7, 12.9, 16.1 and 19.4 for the core diameters of 30, 40, 50 and 60 μm, respectively.

To demonstrate that these multimode fibers also support the transmission of diffraction-limited beams at high power, we have performed experiments at the maximum output power of the available fiber laser. This was performed with the fiber with a core diameter of 60 μm, since the largest core diameter offers the highest SRS threshold. The fiber had a length of 100 m in order to still guarantee for a nearly diffraction-limited beam quality at the exit of the fiber. We were able to transmit a beam with 1013 W of power without the onset of SRS. The SRS power threshold was determined to be 1020 W, while still maintaining

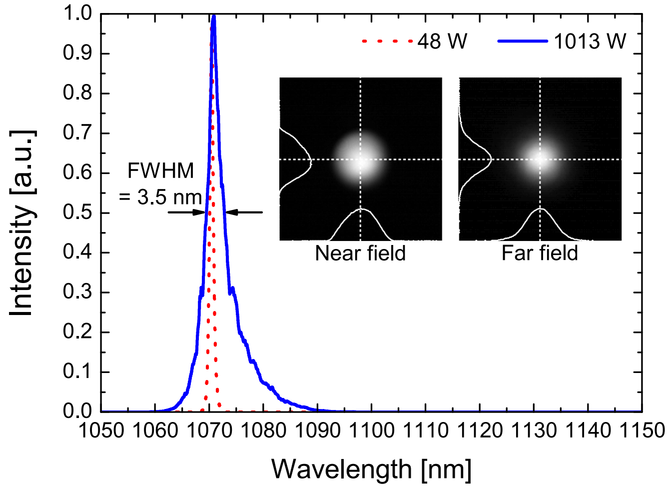

Fig. 5. Measured spectra of the beam which was transmitted through 100 m of fiber with a core diameter of 60 μm at output powers of 48 W and 1013 W. Insets: Near and far field intensity distributions of the output beam at an output power of 1013 W.

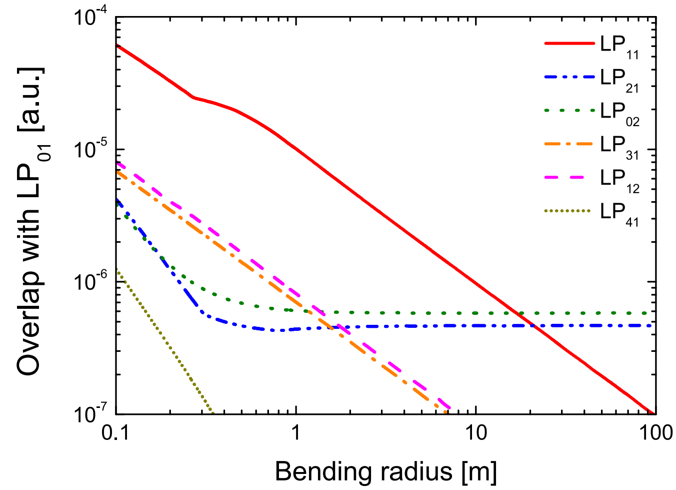

Fig. 6. Calculated overlap between the LP_{01} and several higher-order modes at a wavelength of 1070 nm as function of the bending radius of the fiber with a core diameter of 30 μm (for the sake of clarity only the overlaps with the first six higher-order modes are shown).

a nearly diffraction-limited beam quality. The M^2 was measured to be almost constant (within the accuracy of the measurement) and amounted 1.24 ± 0.06 and 1.32 ± 0.07 at output powers of 48 W and 1013 W, respectively.

The corresponding spectra of the transmitted beam are shown in Fig. 5. With increasing power from 48 W to 1013 W the spectrum broadens gradually. However, the spectral emission bandwidth measured is 3.5 nm (FWHM). This beam delivery system is therefore perfectly suitable for typical high-power industrial applications, which can be further corroborated by the near and far field intensity profiles (see insets Fig. 5) illustrating the good beam quality after transmission of 1013 W of power.

VI. Discussion

The experimentally observed increase of the M^2 along the length of the propagation can be explained by considering Marcuse's coupled power equations [16]

$$\frac{dP_\mu}{dz} = -\alpha_\mu P_\mu + \sum_{\nu \neq \mu} d_{\mu\nu}(P_\nu - P_\mu), \tag{2}$$

which describe the evolution of the power P of mode μ along the propagation distance z. Here $d_{\mu\nu}$ is the coupling coefficient between mode μ and mode ν, and α is the propagation loss [15], [16], [19]. It is stated in the literature [7], [18], [21] that the coupling coefficient $d_{\mu\nu}$ reduces rapidly with mode spacing and is inversely proportional to the fourth power of Δn_{eff}, however, Hurand *et al.* [6] have shown a much weaker dependence on the mode spacing. This inconsistency found in the literature most certainly arises due to the random nature of mode coupling in such highly multimode systems.

Besides the mode spacing the coupling also depends on the overlap of the field distributions of each fiber mode [15], which itself heavily depends on the experimental conditions as shown in Fig. 6. For large bending radii approaching infinity, which corresponds to a straight fiber, the overlap of the fundamental LP_{01}-mode with the LP_{02} is much higher than with the LP_{11}. Indeed, the overlap between LP_{01} and all radially symmetric modes is high in this case. However, with decreasing bending radius the overlap of the fundamental mode to the LP_{11} strongly increases. Since most of our fiber is in this experimental configuration, i.e. with a bending radius in the range of 50 cm and Δn_{eff} between LP_{01} and LP_{11} is the smallest, the coupling to the LP_{11} is dominant.

It is known that mode coupling is a highly complex process with several impact factors. Due to this complex nature and the large number of modes in our highly multimode system, we focused our study on the dependence of the coupling coefficient $d_{\mu\nu}$ on the mode spacing Δn_{eff}. Therefore, the relation

$$d_{\mu\nu} = A \cdot \Delta n_{\text{eff},\mu\nu}^{-B} \tag{3}$$

was substituted into Eq. (2) to fit the theoretically calculated values of M^2 to the experimental results by means of the least squares error with the fit parameters A and B.

To calculate the M^2 values of the beams after the transmission of the beam through the investigated fibers, the same procedure used in our previous work [9] was followed, since for the long fiber lengths and the broad spectrum of our fiber laser the applied incoherent superposition is valid [36]. Hence, the resulting intensity distributions in the transverse xy-plane in the near and far field of the beam that is emitted from the fiber with the length L were calculated with

$$I_{\text{N}}(x, y, L) = \sum_{\mu=1}^{m} P_\mu(L) \cdot \frac{I_{\mu,\text{N}}(x, y, L)}{\iint I_{\mu,\text{N}}(x, y, L)dxdy} \tag{4}$$

and

$$I_{\text{F}}(x, y, L) = \sum_{\mu=1}^{m} P_\mu(L) \cdot \frac{I_{\mu,\text{F}}(x, y, L)}{\iint I_{\mu,\text{F}}(x, y, L)dxdy}, \tag{5}$$

where m is the number of modes supported by the fiber and $P_\mu(L)$ is the power of each mode μ as calculated from Eq. (2).

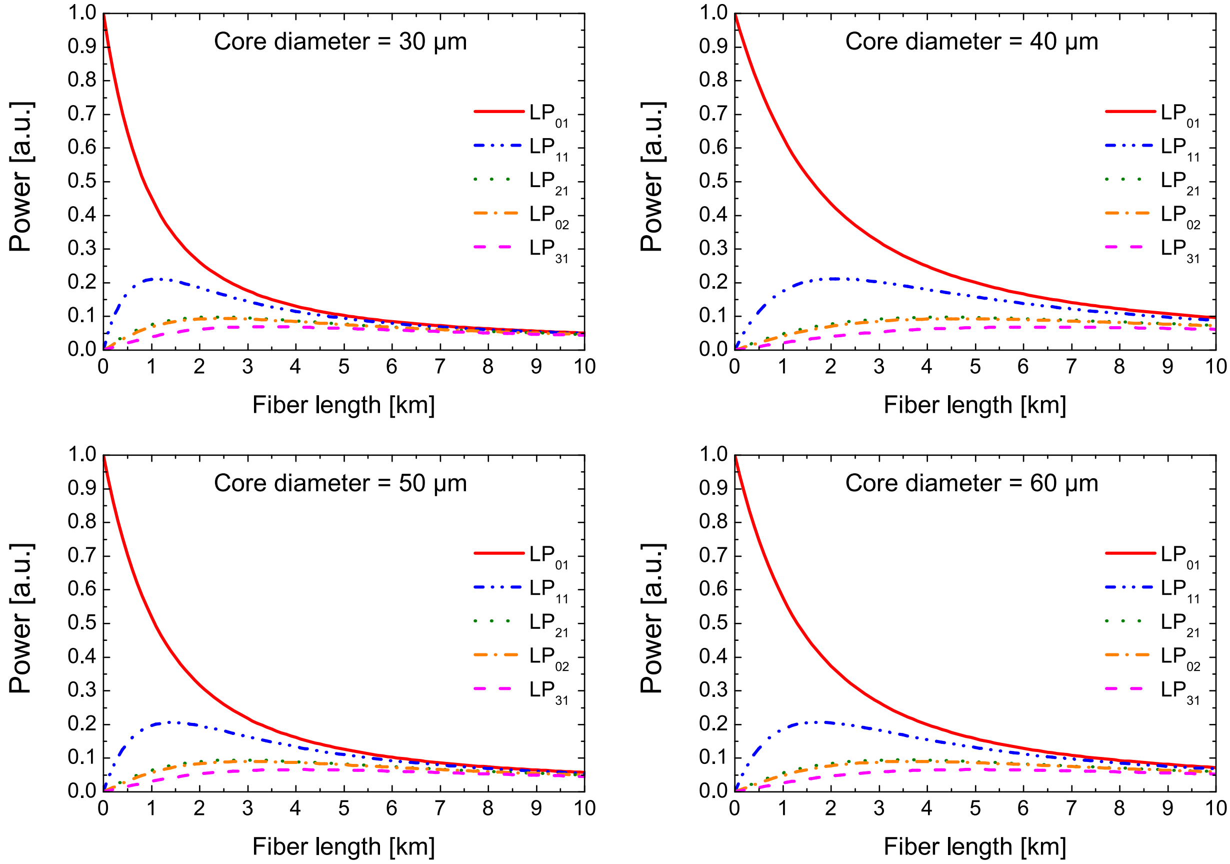

Fig. 7. Calculated evolution of modal powers along the propagation in the fibers with core diameters of 30, 40, 50 and 60 μm (for the sake of clarity only the first five modes are shown).

TABLE I
FIT PARAMETERS A AND B FOR EACH CORE DIAMETER

d_{core}	A	B
30 µm	$5.97 \cdot 10^{-11}$	1.94
40 µm	$9.20 \cdot 10^{-12}$	1.96
50 µm	$8.18 \cdot 10^{-12}$	1.92
60 µm	$3.11 \cdot 10^{-12}$	1.93

The losses were neglected in our calculations and it is assumed that only the fundamental LP_{01}-mode is launched at the entrance of the fiber. The propagation constants $n_{\text{eff},\mu}$ of each fiber mode μ and their corresponding near and far field intensity distributions $I_{\mu,N}(x, y, L)$ and $I_{\mu,F}(x, y, L)$ were calculated by solving the wave equation using MATLAB. Finally, the resulting near and far field distributions given by Eqs. (4) and (5) were used to calculate the M^2 values for each fiber length L according to the second moment method [37]. The evolution of the modal powers and the resulting M^2 values are shown in Fig. 7 and Fig. 8, respectively.

Table I shows the fit parameters A and B for each core diameter. Whereas A is decreasing with increasing core diameter, B is almost constant at an average value of 1.94. Hence considering Eq. (3), the coupling coefficient $d_{\mu\nu}$ reduces with mode spacing, but this dependency is, as Hurand *et al.* [6] already stated, weaker than suggested in the literature [7], [18], [21] and is rather reciprocally proportional to the second power of Δn_{eff}.

It can be seen in Fig. 7 that the power is gradually transferred from the LP_{01}, which initially contains 100% of the power, to all higher-order modes and that an equilibrium state is reached after a certain fiber length. This shows that even though the coupling itself is not homogeneous across all modes, since in a step-index fiber the mode spacing is not equidistant [30], the equilibrium energy distribution between all modes is homogeneous. The coupling from the LP_{01} to the LP_{11}-mode is dominant since they are separated by the smallest Δn_{eff}. The overall behavior is similar for all examined fibers with different core diameters, suggesting that the coupling mechanism in all fibers is the same.

The comparison between the experimentally measured M^2 values and the calculations are given in the graph on the left (see Fig. 8(a)). According to the graph on the right (see Fig. 8(b)), the equilibrium state is reached after a couple of tens of kilometers for a core diameter of 30 μm, which results in a top-hat intensity distribution since all modes superpose incoherently. The corresponding M^2 value of 9.3 is consistent with previously stated nominal beam quality factor of 9.7. For the larger core diameters of 40, 50 and 60 μm the equilibrium state is reached only after a propagation length of beyond 100 km. According to the method proposed by Savović *et al.* [38], which is based

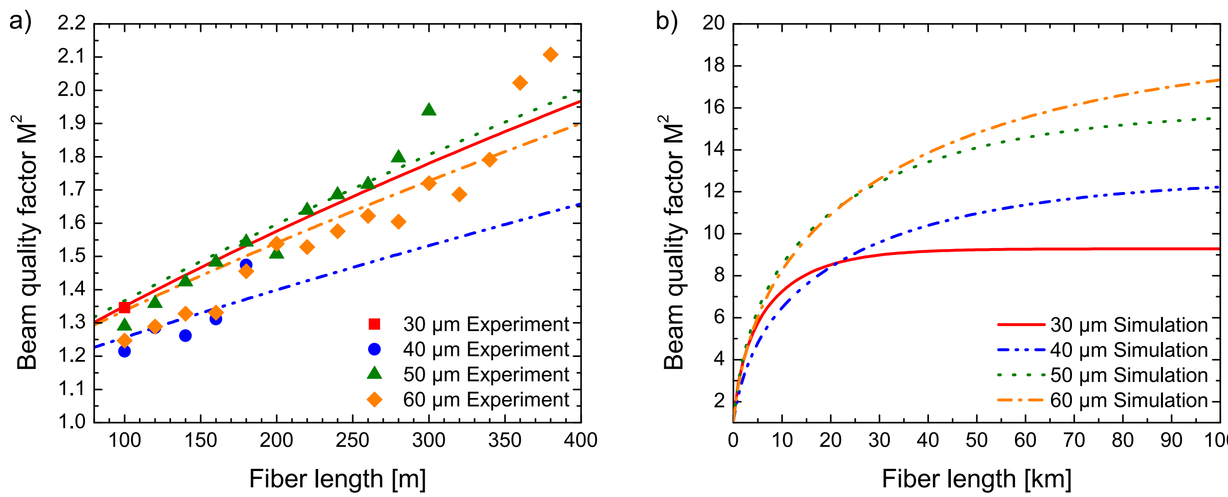

Fig. 8. Calculated beam quality factor M^2 as a function of the fiber length. (a) For fiber lengths between 80 and 400 m including the experimental results from Fig. 4. (b) For fiber lengths between 0 and 100 km.

on Gloge's power flow equation [18], together with the approximation that the launched beam has an M^2 close to unity [6] the beam quality factor

$$M^2 = \frac{2\pi \cdot n_{\text{core}} \cdot w_0 \cdot \sqrt{2LD}}{\lambda} \tag{6}$$

is found to scale with the square root of the fiber length L. Here D is the global coupling coefficient as defined in [38], n_{core} is the refractive index of the core, and w_0 is the waist radius of beam at the fiber output [6]. In comparison to the approximations of Fermann [7], Hurand *et al.* [6] confirmed Eq. (1) qualitatively but stated that the dependency on the core and cladding diameter is weaker. From their findings it can be concluded that

$$M^2 \propto \frac{d_{\text{core}}}{d_{\text{clad}}} \cdot \sqrt{L}, \tag{7}$$

which is valid for short fibers where just a few modes are excited and which is far from the equilibrium state. For a preform with a constant ratio between the diameters of core and cladding, the beam quality scales with the square root of the fiber length and is independent of the size of the core or the cladding, which is in good agreement with the results presented here.

VII. Conclusion

In this work we have analyzed the requirements for preserving a good beam quality in highly multimode fibers by using the coupled mode theory as a framework for the fiber design to reduce mode coupling. This was experimentally verified with a fully monolithic setup using beam delivery fibers with an NA of 0.22. A nearly diffraction-limited beam quality ($M^2 \approx 1.3$) was maintained over a fiber length of 100 m for core diameters of up to 60 μm. It was further presented that the beam quality factor M^2 degrades gradually with increasing fiber length, but still remains at a useful value of 2.1 for a fiber with a core diameter of 60 μm and a length of 380 m. The power capability was demonstrated by the transmission of a nearly diffraction-limited high-power beam with a power of 1 kW through a 100 m long fiber with a core diameter of 60 μm without the onset of SRS. Further research will be devoted to the investigation of the beam delivery at even higher laser output powers, which are especially relevant for material processing applications like cutting or remote welding.

Acknowledgment

The authors would like to thank F. Beirow and P. Weinert for support in the experiments and fruitful discussions.

References

[1] D. J. Richardson, J. Nilsson, and W. A. Clarkson, "High power fiber lasers: Current status and future perspectives," *J. Opt. Soc. Amer. B*, vol. 27, no. 11, pp. B63–B92, 2010.
[2] J. W. Dawson *et al.*, "Analysis of the scalability of diffraction-limited fiber lasers and amplifiers to high average power," *Opt. Express*, vol. 16, no. 17, pp. 13240–13266, 2008.
[3] R. G. Smith, "Optical power handling capacity of low loss optical fibers as determined by stimulated Raman and Brillouin scattering," *Appl. Opt.*, vol. 11, no. 11, pp. 2489–2494, 1972.
[4] M. Abdou Ahmed and A. Voss, "Optical fibres for high-power single-mode beam delivery," *Optik Photonik*, vol. 7, no. 2, pp. 38–43, 2012.
[5] C. D. Stacey, R. M. Jenkins, J. Banerji, and A. R. Davies, "Demonstration of fundamental mode only propagation in highly multimode fibre for high power EDFAs," *Opt. Commun.*, vol. 269, no. 2, pp. 310–314, 2007.
[6] S. Hurand, L.-A. Chauny, H. El-Rabii, S. Joshi, and A. P. Yalin, "Mode coupling and output beam quality of 100–400 μm core silica fibers," *Appl. Opt.*, vol. 50, no. 4, pp. 492–499, 2011.
[7] M. E. Fermann, "Single-mode excitation of multimode fibers with ultrashort pulses," *Opt. Lett.*, vol. 23, no. 1, pp. 52–54, 1998.
[8] M. Vogel, *Specialty Fibers for High Brightness Laser Beam Delivery*, ser. Laser in der Materialbearbeitung. Munich, Germany: Herbert Utz Verlag, 2014.
[9] C. Röhrer, G. Kleem, M. Abdou Ahmed, and T. Graf, "Analysis of fundamental-mode beam transport in highly multimode fibers," *J. Lightw. Technol.*, vol. 35, no. 17, pp. 3637–3642, Sep. 2017.
[10] S. Shaklan, "Measurement of intermodal coupling in weakly multimode fibre optics," *Electron. Lett.*, vol. 26, no. 24, pp. 2022–2024, 1990.
[11] S. Shaklan, "Selective mode injection and observation for few-mode fiber optics," *Appl. Opt.*, vol. 30, no. 30, pp. 4379–4383, 1991.
[12] J.-P. Negel *et al.*, "Delivery of 800 W of nearly diffraction-limited laser power through a 100 m long multi-mode fiber," *Laser Phys. Lett.*, vol. 11, no. 5, 2014, Art. no. 055104.

[13] R. Brüning, Y. Zhang, M. McLaren, M. Duparré, and A. Forbes, "Overlap relation between free-space Laguerre Gaussian modes and step-index fiber modes," *J. Opt. Soc. Amer. A*, vol. 32, no. 9, pp. 1678–1682, 2015.
[14] R. Olshansky, "Propagation in glass optical waveguides," *Rev. Mod. Phys.*, vol. 51, no. 341, pp. 341–367, 1979.
[15] D. Marcuse, *Theory of Dielectric Optical Waveguides*, ser. Quantum Electronics - Principles and Applications, 2nd ed. Boston, MA, USA: Academic, 1991.
[16] D. Marcuse, "Derivation of coupled power equations," *Bell Syst. Tech. J.*, vol. 51, no. 1, pp. 229–237, 1972.
[17] D. Marcuse, "Coupled mode theory of round optical fibers," *Bell Syst. Tech. J.*, vol. 52, no. 6, pp. 817–842, 1973.
[18] D. Gloge, "Optical power flow in multimode fibers," *Bell Syst. Tech. J.*, vol. 51, no. 8, pp. 1767–1783, 1972.
[19] K.-P. Ho and J. M. Kahn, "Mode coupling and its impact on spatially multiplexed systems," in *Optical Fiber Telecommunications*. Amsterdam, The Netherlands: Elsevier, 2013, pp. 491–568.
[20] D. Marcuse, "Mode conversion caused by surface imperfections of a dielectric slab waveguide," *Bell Syst. Tech. J.*, vol. 48, no. 10, pp. 3187–3215, 1969.
[21] R. Olshansky, "Distortion losses in cabled optical fibers," *Appl. Opt.*, vol. 14, no. 1, pp. 20–21, 1975.
[22] A. F. Garito, J. Wang, and R. Gao, "Effects of random perturbations in plastic optical fibers," *Science*, vol. 281, no. 5379, pp. 962–967, 1998.
[23] R. Lingle, D. Peckham, A. H. McCurdy, and J. Kim, "Light-guiding fundamentals and fiber design," in *Specialty Optical Fibers Handbook*. Cambridge, MA, USA: Academic, 2007, pp. 19–68.
[24] F. Mitschke, *Glasfasern Physik und Technologie*. Heidelberg, Germany: Spektrum Akademischer Verlag, 2005.
[25] R. B. Runk, "A zirconia induction furnace for drawing precision silica wave guides," in *Proc. Topical Conf. Opt. Fiber Transmiss. II*, Williamsburg, VA, USA, 1977, p. TuB5.
[26] D. B. Keck, "Optical Fiber Waveguides," in *Fundamentals of Optical Fiber Communications*, 2nd ed. New York, NY, USA: Academic, 1981, pp. 1–107.
[27] D. Gloge, "Optical-fiber packaging and its influence on fiber straightness and loss," *Bell Syst. Tech. J.*, vol. 54, no. 2, pp. 245–262, 1975.
[28] K. Nagano and S. Kawakami, "Mode conversion coefficients in graded-index fibers with various fiber-coating schemes measurements," *Appl. Opt.*, vol. 21, no. 3, pp. 542–546, 1982.
[29] Y.-C. Yang, H.-L. Lee, and H.-M. Chou, "Elasto-optics in double-coated optical fibers induced by axial strain and hydrostatic pressure," *Appl. Opt.*, vol. 41, no. 10, pp. 1989–1994, 2002.
[30] A. W. Snyder and J. D. Love, *Optical Waveguide Theory*. Boston, MA, USA: Springer, 1983.
[31] D. Marcuse, "Mode conversion in optical fibers with monotonically increasing core radius," *J. Lightw. Technol.*, vol. LT-5, no. 1, pp. 125–133, Jan. 1987.
[32] J. D. Love, "Application of a low-loss criterion to optical waveguides and devices," in *IEE Proc. J.—Optoelectron.*, vol. 136, no. 4, 1989, pp. 225–228.
[33] J. D. Love, W. M. Henry, W. J. Stewart, R. J. Black, S. Lacroix, and F. Gonthier, "Tapered single-mode fibres and devices. Part 1: Adiabaticity criteria," in *IEE Proc. J.—Optoelectron.*, vol. 138, no. 5, 1991, pp. 343–354.
[34] A. D. Yablon, *Optical Fiber Fusion Splicing*, ser. Optical Sciences. Berlin, Germany: Springer-Verlag, 2005.
[35] R. Paschotta, "The Photonics Spotlight: Beam Quality Limit for Multimode Fibers," RP Photonics Consulting GmbH, Bad Dürrheim, Germany. Nov. 12, 2013. [Online]. Available: https://www.rp-photonics.com/spotlight_2013_11_12.html, Accessed Nov. 16, 2018.
[36] S. Wielandy, "Implications of higher-order mode content in large mode area fibers with good beam quality," *Opt. Express*, vol. 15, no. 23, pp. 15402–15409, 2007.
[37] Lasers and laser-related equipment - test methods for laser beam widths, divergence angles and beam propagation ratios, ISO 11146, 2005.
[38] S. Savović and A, Djordjevich, "Method for calculating the coupling coefficient in step-index optical fibers," *Appl. Opt.*, vol. 46, no. 9, pp. 1477–1481, 2007.

Christian Röhrer received the B.Sc. degree from Ravensburg-Weingarten University of Applied Sciences, Weingarten, Germany, in 2012, the B.Sc. degree from Nottingham Trent University, Nottingham, U.K., in 2012, and the M.Sc. degree from Darmstadt University of Applied Sciences, Darmstadt, Germany, in 2014. Since 2014, he has been working toward the Ph.D. degree with the Institut für Strahlwerkzeuge, University of Stuttgart, Stuttgart, Germany, within the framework of the Graduate School of Excellence advanced Manufacturing Engineering. His research interests include modeling and experimental characterization of optical fibers including the fiber drawing and fiber handling for high-brightness laser beam delivery.

Christophe A. Codemard received the Graduate degree in optoelectronics from École Nationale Supérieure des Sciences Appliquées et de Technologie, Lannion, France, in 1999, and the Ph.D. degree from the Optoelectronics Research Centre, Southampton University, Southampton, U.K., in 2007. Since 2011, he has led the Advanced Laser Laboratory of SPI Lasers UK Ltd, Southampton, U.K. His main research interests include high power rare-earth doped fiber lasers and amplifiers, pulsed fiber lasers, nonlinear effects, and numerical simulations. He has published more than 150 papers in scientific journals and conference proceedings and is a Senior Member of the Optical Society of America.

Götz Kleem graduated as a Chemical-Production-Worker from Hoechst AG, Offenbach, Germany, in 1987, and as a State Certified Technician specialized in chemical technique in 2009. In 1994, he performed an internal job change to work in the office for production, he led this as an Office-Administrator, from 1997 to 2009. In 2010, he joined the Institut für Strahlwerkzeuge, University of Stuttgart, Stuttgart, Germany, where he took over the production of fiber preforms and optical fibers.

Thomas Graf received the M.Sc. degree in physics and the Ph.D. degree from the University of Berne, Berne, Switzerland, in 1993 and 1996, respectively. After 15 months of research with Strathclyde University, Glasgow, U.K., he returned to the University of Berne in April 1999, where he was awarded the Venia Docendi in 2001 and where he was appointed Assistant Professor in April 2002. Since June 2004, he has been full University Professor and Director of the Institut für Strahlwerkzeuge, University of Stuttgart, Stuttgart, Germany.

Marwan Abdou Ahmed received the Diplôme d'Etudes Approfondies and the Ph.D. degree from the University of Saint-Etienne, Saint-Etienne, France, in 1999 and 2003, respectively. He received the Habilitation degree for the University Paris-Sud XI, Orsay, France, in May 2012. In 2004, he joined the Institut für Strahlwerkzeuge, University of Stuttgart, Stuttgart, Germany, working mainly on the development of polarization and wavelength selective optics for high-power solid-state lasers. Since June 2011, he has been responsible for the "Laser Development and Laser Optics" department, Institut für Strahlwerkzeuge. He and his team are focusing on ultrafast and high-power thin-disk laser systems as well as on temporal and spatial beam shaping optics. He has been engaged in and has coordinated several national and EU projects.